SATURATION AND RELIABLE HIERARCHICAL A POSTERIORI MORLEY FINITE ELEMENT ERROR CONTROL*

Carsten Carstensen

Humboldt-Universität zu Berlin, Institut für Mathematik, Unter den Linden 6, 10099 Berlin, Germany
Email: cc@math.hu-berlin.de

Dietmar Gallistl

Department of Applied Mathematics, University of Twente, P.O. Box 217, 7500 AE Enschede
The Netherlands
Email: d.gallistl@utwente.nl

Yunqing Huang

Institute for Computational and Applied Mathematics and Hunan Key Laboratory for Computation &
Simulation in Science & Engineering, Xiangtan University, Human 411105, China
Email: huangyq@xtu.edu.cn

Abstract

This paper proves the saturation assumption for the nonconforming Morley finite element discretization of the biharmonic equation. This asserts that the error of the Morley approximation under uniform refinement is strictly reduced by a contraction factor smaller than one up to explicit higher-order data approximation terms. The refinement has at least to bisect any edge such as red refinement or 3-bisections on any triangle.

This justifies a hierarchical error estimator for the Morley finite element method, which simply compares the discrete solutions of one mesh and its red-refinement. The related adaptive mesh-refining strategy performs optimally in numerical experiments. A remark for Crouzeix-Raviart nonconforming finite element error control is included.

Mathematics subject classification: 65M12, 65M60, 65N25.
Key words: Saturation, Hierarchical error estimation, Finite element, Nonconforming, Biharmonic, Morley, Kirchhoff plate, Crouzeix-Raviart.

1. Introduction

The saturation assumption is made in many engineering finite element applications and is often observed in the asymptotic regime for very fine meshes. The mathematical justification is less obvious and often requires restrictions on the mesh-refinement and on extra data oscillations or data approximation terms. Given the two finite element approximations u_H and u_h with respect to a coarse mesh $\mathcal{T}_H$ and its overall refinement $\mathcal{T}_h$ to the exact solution u, the errors in the broken energy norm $\|\bullet\|_{\text{NC}}$ (with respect to piecewise Sobolev norms) satisfies

$$\|u - u_h\|_{\text{NC}} \leq \varrho \|u - u_H\|_{\text{NC}} + C \, \text{data apx}(\mathcal{T}_H). \tag{1.1}$$

with positive constants $\varrho < 1$ and $C < \infty$. The data approximation terms data apx$(\mathcal{T}_H)$ read $\|H^\alpha f\|$ for the given right-hand side $f \in L^2(\Omega)$ of the PDE in the L^2 norm $\|\bullet\|$ over the domain Ω weighted by the piecewise constant mesh-size H. They can be evaluated explicitly and reflect the mesh-refinement to resolve the local mesh refinement through the variable mesh-size H and

are of higher order with $\alpha = 2$ for the Morley and with $\alpha = 1$ of first-order for the Crouzeix-Raviart finite element method. Those terms are efficient in the sense data $\mathrm{apx}(\mathcal{T}_H)$ is controlled by the error $\|u - u_h\|_{\mathrm{NC}}$ plus data oscillation terms like $\|H^\alpha(f - \Pi_0 f)\|$ with the piecewise integral means $\Pi_0 f$ of f. It is known that $\|H^\alpha(f - \Pi_0 f)\|$ can dominate the error and even $u_H = u_h$ is possible for highly oscillating data $f \in L^2(\Omega)$ in a possibly very large computational regime which makes (1.1) less useful, so this paper aims at applications for piecewise smooth data when this term is negligible. Saturation results of the type (1.1) are justified for the conforming finite element method [5, 12], where counterexamples are characterized for very coarse meshes when (1.1) fails even for a constant right-hand side.

In contrast to [12] for conforming FEMs and second-order problems, this paper asserts saturation for uniform mesh-refinement rather than for an increased polynomial degree. For conforming finite elements for the Poisson equation, (1.1) was recently characterized in [5]. It came as a surprise to the authors that there are no restrictions on the mesh for the nonconforming Morley or Crouzeix-Raviart finite element schemes as all. Moreover, for those schemes, the main result (1.1) of this paper is not restricted to newest-vertex bisection or red-green-blue refinement, but is also valid for more exotic refinement strategies as long as the family $\mathbb{T}$ of triangulations under consideration is shape regular—so unstructured grids with local mesh-refining are included.

An immediate consequence of saturation is hierarchical error control with a justification via a triangle inequality. This and (1.1) imply

$$\|u - u_H\|_{\mathrm{NC}} \leq \|u - u_h\|_{\mathrm{NC}} + \|u_H - u_h\|_{\mathrm{NC}} \leq \varrho \|u - u_H\|_{\mathrm{NC}} + \eta + \mu$$

for the hierarchical error estimator $\eta := \|u_H - u_h\|_{\mathrm{NC}}$ and the data approximation term $\mu := C \, \mathrm{data} \, \mathrm{apx}(\mathcal{T}_H)$. Since $\varrho < 1$, this is reliability in the form

$$\|u - u_H\|_{\mathrm{NC}} \leq C_{\mathrm{rel}}(\eta + \mu) \quad \text{with reliability constant } C_{\mathrm{rel}} := 1/(1 - \varrho). \tag{1.2}$$

The point is that (1.2) is *not* an asymptotic result and holds for all coarse meshes $\mathcal{T}_H$ with the extra cost of calculating u_h with respect to a uniform refinement $\mathcal{T}_h$ thereof. Moreover, the regularity of the exact solution does not enter at all and the higher-order term μ depends explicitly on the data and can be computed. In conclusion, this paper justifies hierarchical error control in the form

$$\|u - u_H\|_{\mathrm{NC}} \leq C_1 \|u_h - u_H\|_{\mathrm{NC}} + C_2 \mathrm{data} \, \mathrm{apx}(\mathcal{T}_H) \tag{1.3}$$

with universal reliability constants C_1 and C_2. The estimate (1.3) serves as a basis of further more local versions of hierarchical error control with less computational costs as outlined in [29] for conforming finite elements in second-order problems.

The remaining parts of this paper are organized as follows. Section 2 establishes the notation and the main saturation result (1.1) for the biharmonic equation with homogeneous boundary conditions and its numerical simulation with the Morley finite element method. The arguments rely on a new discrete efficiency and a known quasi-orthogonality estimate. Section 3 states the hierarchical error control (1.3) for the Morley finite element method, which is exemplified in numerical experiments in Section 4. Some comments on the second-order Poisson model problem and its numerical simulation with the Crouzeix-Raviart finite element method in Section 5 conclude the paper.

The results are given in two space dimensions for the simplicity of the presentation but are expected to carry over in higher space dimensions.

Standard notation on Lebesgue and Sobolev spaces applies and $(\cdot, \cdot)_{L^2(\Omega)}$ denotes the L^2 inner product with norm $\|\cdot\| := \|\cdot\|_{L^2(\Omega)}$ over the domain Ω.

The integral mean is denoted by $\fint$. The dot $\cdot$ denotes the product of two one-dimensional lists of the same length while the colon denotes the Euclidean product of matrices, e.g., $a \cdot b = a^\top b \in \mathbb{R}$ for $a, b \in \mathbb{R}^2$ and $A : B = \sum_{j,k=1}^2 A_{jk} B_{jk}$ for 2×2 matrices A, B.

The notation $a \lesssim b$ abbreviates $a \le Cb$ for a positive generic constant C that does not depend on the mesh-size. The notation $a \approx b$ stands for $a \lesssim b \lesssim a$.

The piecewise constant mesh-size function $h \in P_0(\mathcal{T}_h)$ is defined by $h|_T := |T|^{1/2}$ for any triangle T of area $|T|$ in $\mathcal{T}_h$. The L^2 projection onto piecewise constants with respect to a mesh $\mathcal{T}_h$ with mesh-size function h is denoted by $\Pi_{0,h}$. The measure $|\cdot|$ is context-sensitive and refers to the length of an edge or the area of some domain or the modulus of a real number or the Euclidean length of a vector.

Figure 1.1. Mnemonic diagrams of the Morley FEM (left) and the Crouzeix-Raviart FEM (right).

2. The Saturation Property for the Morley FEM

Given $f \in L^2(\Omega)$, the biharmonic problem seeks $u \in H^2(\Omega)$ with

$$\Delta^2 u = f \quad \text{in } \Omega \quad \text{and} \quad u = \frac{\partial u}{\partial \nu} = 0 \quad \text{on } \partial\Omega.$$

Its weak form incorporates the boundary conditions in the space $V := H_0^2(\Omega)$ and then seeks $u \in V$ with

$$(D^2 u, D^2 v)_{L^2(\Omega)} = (f, v)_{L^2(\Omega)} \quad \text{for all } v \in V. \tag{2.1}$$

Given a regular triangulation $\mathcal{T}_h$ of the bounded Lipschitz domain Ω with polygonal boundary $\partial\Omega$ into triangles with the set of edges $\mathcal{F}_h$ and the set of vertices $\mathcal{N}_h$, let $\mathcal{F}_h(\Omega)$ and $\mathcal{N}_h(\Omega)$ denote the sets of interior edges and interior vertices. Throughout the paper, $P_k(\mathcal{T}_h)$ denotes the space of piecewise polynomials with respect to $\mathcal{T}_h$ of degree $\le k$ and ∇_{NC} (resp. D_{NC}^2) denotes the piecewise action of the gradient (resp. the Hessian). The Morley finite element space [23] reads

$$M(\mathcal{T}_h) := \left\{ v \in P_2(\mathcal{T}_h) \,\middle|\, \begin{array}{l} v \text{ is continuous at } \mathcal{N}_h(\Omega) \text{ and vanishes at } \mathcal{N}_h(\partial\Omega); \\ \nabla_{\mathrm{NC}} v \text{ is continuous at the interior edges' midpoints} \\ \text{and vanishes at the midpoints of the edges of } \partial\Omega \end{array} \right\}.$$

The Morley finite element discretisation of (2.1) seeks $u_h \in M(\mathcal{T}_h)$ with

$$(D_{\mathrm{NC}}^2 u_h, D_{\mathrm{NC}}^2 v_h)_{L^2(\Omega)} = (f, v_h)_{L^2(\Omega)} \quad \text{for all } v_h \in M(\mathcal{T}_h). \tag{2.2}$$

A priori error estimates (such as (2.3) below) are proved in [16, 21, 27]. The Morley FEM was also studied with regard to its superconvergence [9, 18], lower discretization error bounds [22], eigenvalue problems [25], and lower eigenvalue bounds [4, 17, 30]. Furthermore, there are

modified versions of the Morley FEM for singular perturbation problems [10, 24] or anisotropic meshes [26].

Let $\mathbb{T}$ denote a family of shape-regular triangulations of Ω. A triangulation $\mathcal{T}_h \in \mathbb{T}$ is called a uniform refinement of $\mathcal{T}_H \in \mathbb{T}$ if $\mathcal{T}_h$ is a refinement of $\mathcal{T}_H$ by the (successive) application of some refinement rule that bisects each edge in $\mathcal{F}_H$. The main result verifies (1.1) for the Morley finite element method.

Theorem 2.1 (saturation) *There exist mesh-size independent constants $0 < \rho < 1$ and $0 < C < \infty$ which depend on $\mathbb{T}$ but neither on any mesh-size nor on any number of triangles such that the following holds. Let $\mathcal{T}_h \in \mathbb{T}$ be a uniform refinement of the regular triangulation $\mathcal{T}_H \in \mathbb{T}$ with mesh-size function $H \in P_0(\mathcal{T}_H)$. The discrete solutions $u_H \in M(\mathcal{T}_H)$ and $u_h \in M(\mathcal{T}_h)$ satisfy*

$$\|D_{\mathrm{NC}}^2(u - u_h)\|^2 \leq \rho\,\|D_{\mathrm{NC}}^2(u - u_H)\|^2 + C\,\|H^2 f\|^2.$$

Classical a priori error estimates [21, 27] state linear convergence

$$\|D_{\mathrm{NC}}^2(u - u_h)\| \leq Ch\,(\|u\|_{H^3(\Omega)} + h\|f\|) \tag{2.3}$$

and one observes that the term $C\,\|H^2 f\|^2$ in Theorem 2.1 is of higher order under uniform mesh-refinement compared with the piecewise constant approximation of the Hessian. The required H^3 regularity for the a priori estimate (2.3) is for example satisfied if Ω is convex [3, 14].

The remaining parts of this section are devoted to the proof of Theorem 2.1. The proof analyzes the explicit residual-based error estimator from [1, 19]. The unit tangent vector of an edge E is denoted by τ_E. For any interior edge $E \in \mathcal{F}_h(\Omega)$, there exist two adjacent triangles T_+ and T_- such that $E = \partial T_+ \cap \partial T_-$. Given any (possibly vector-valued) function v, define the jump of v across E by $[v]_E := v|_{T_+} - v|_{T_-}$. Let for each edge $E \in \mathcal{F}_h$, the edge-patch be denoted by

$$\omega_{E,h} := \mathrm{int}(\bigcup\{T \in \mathcal{T}_h \mid E \text{ is an edge of } T\}).$$

The explicit residual-based error estimator reads

$$\eta_h^2 := \sum_{T \in \mathcal{T}_h} \left(|T|^2 \|f\|_{L^2(T)}^2 + \sum_{E \in \mathcal{F}(T)} |E|\,\|[D_{\mathrm{NC}}^2 u_h]_E \tau_E\|_{L^2(E)}^2 \right).$$

The global error estimator η_h is known [1, 19] to be reliable in the sense that there exists a mesh-size independent constant C_{rel} such that

$$\|D_{\mathrm{NC}}^2(u - u_h)\|^2 \leq C_{\mathrm{rel}}\eta_h^2. \tag{2.4}$$

The proof of Theorem 2.1 is based on the following two lemmas. The first lemma states quasi-orthogonality which has been proven by [20] and [13].

Lemma 2.1 (quasi-orthogonality, Lemma 3.4 of [20]) *Let $\mathcal{T}_h \in \mathbb{T}$ be a uniform refinement of $\mathcal{T}_H \in \mathbb{T}$. The discrete solutions $u_H \in M(\mathcal{T}_H)$ and $u_h \in M(\mathcal{T}_h)$ satisfy for a constant $C_{\mathrm{qo}} \approx 1$ that*

$$|(D_{\mathrm{NC}}^2(u - u_h), D_{\mathrm{NC}}^2(u_h - u_H))_{L^2(\Omega)}| \leq C_{\mathrm{qo}} \sum_{T \in \mathcal{T}_H \setminus \mathcal{T}_h} |T|\,\|f\|_{L^2(T)}\|D_{\mathrm{NC}}^2(u - u_h)\|_{L^2(T)}.$$

The second lemma states discrete efficiency of edge-residuals. This notion of discrete efficiency was first introduced by [8] for second-order problems. The version stated here for the Morley FEM appears to be new.

Lemma 2.2 (discrete efficiency) *Let $\mathfrak{T}_h \in \mathbb{T}$ be a uniform refinement of $\mathfrak{T}_H \in \mathbb{T}$ with discrete solutions $u_h \in M(\mathfrak{T}_h)$ and $u_H \in M(\mathfrak{T}_H)$. Any edge $E \in \mathcal{F}_H$ in the coarser triangulation satisfies the discrete efficiency*

$$|E| \, \|[D_{\mathrm{NC}}^2 u_H]_E \tau_E\|_{L^2(E)}^2 \lesssim \|D_{\mathrm{NC}}^2(u_h - u_H)\|_{L^2(\omega_{E,H})}^2.$$

Proof. Let $\flat_E \in P_1(\mathfrak{T}_h)$ denote the piecewise affine function with respect to the fine triangulation $\mathfrak{T}_h$ with $\flat_E(\mathrm{mid}(E)) = 2$ and $\flat_E(z) = 0$ for all vertices $z \in \mathcal{N}_h \setminus \{\mathrm{mid}(E)\}$ in the fine triangulation which are different from $\mathrm{mid}(E)$. This discrete bubble function satisfies

$$\mathrm{supp}\,\flat_E = \overline{\omega_{E,H}}, \qquad \|\flat_E\|_{L^\infty(\Omega)} = 2, \quad \text{and} \quad \fint_E \flat_E \, ds = 1.$$

Define $\psi_E := (\flat_E [D_{\mathrm{NC}}^2 u_H]_E \tau_E) \in H_0^1(\omega_{E,H}; \mathbb{R}^2)$. Since $[D_{\mathrm{NC}}^2 u_H]_E$ is constant along E, a direct calculation with the property $\|\flat_E^{1/2}\|_{L^2(E)}^2 = \int_E \flat_E \, ds = |E|$ leads to

$$\|[D_{\mathrm{NC}}^2 u_H]_E \tau_E\|_{L^2(E)}^2 = |E| \, |[D_{\mathrm{NC}}^2 u_H]_E \tau_E|^2 = \|\flat_E^{1/2} [D_{\mathrm{NC}}^2 u_H]_E \tau_E\|_{L^2(E)}^2.$$

The Curl of a vector field $\beta \in H^1(\Omega; \mathbb{R}^2)$ is defined as

$$\mathrm{Curl}\,\beta := \begin{pmatrix} -\partial\beta_1/\partial x_2 & \partial\beta_1/\partial x_1 \\ -\partial\beta_2/\partial x_2 & \partial\beta_2/\partial x_1 \end{pmatrix}.$$

An inverse inequality on the edge-patch $\omega_{E,H}$ proves

$$\|\mathrm{Curl}\,\psi_E\|_{L^2(\omega_{E,H})} = |[D_{\mathrm{NC}}^2 u_H]_E \tau_E| \, \|\mathrm{Curl}\,\flat_E\|_{L^2(\omega_{E,H})} \lesssim |[D_{\mathrm{NC}}^2 u_H]_E \tau_E|. \tag{2.5}$$

An integration by parts reveals

$$\|\flat_E^{1/2} [D_{\mathrm{NC}}^2 u_H]_E \tau_E\|_{L^2(E)}^2 = \int_E \left(\psi_E \cdot [D_{\mathrm{NC}}^2 u_H]_E \tau_E \right) ds$$
$$= \int_{\omega_{E,H}} D_{\mathrm{NC}}^2(u_h - u_H) : \mathrm{Curl}\,\psi_E \, dx.$$

(The last identity follows with the L^2-orthogonality of $\mathrm{Curl}\,\psi_E$ to $D_{\mathrm{NC}}^2 u_h$.) The Cauchy inequality and the inverse estimate (2.5) prove that this is bounded by

$$\|D_{\mathrm{NC}}^2(u_h - u_H)\|_{L^2(\omega_{E,H})} \|\mathrm{Curl}\,\psi_E\|_{L^2(\omega_{E,H})}$$
$$\lesssim \|D_{\mathrm{NC}}^2(u_h - u_H)\|_{L^2(\omega_{E,H})} |[D_{\mathrm{NC}}^2 u_H]_E \tau_E|$$
$$= \|D_{\mathrm{NC}}^2(u_h - u_H)\|_{L^2(\omega_{E,H})} |E|^{-1/2} \|[D_{\mathrm{NC}}^2 u_H]_E \tau_E\|_{L^2(E)}.$$

The combination of the preceding estimates concludes the proof. $\qquad\square$

Proof. [Proof of Theorem 2.1] The reliability (2.4) and the discrete efficiency of Lemma 2.2 together with the finite overlap of edge-patches lead to

$$\|D_{\mathrm{NC}}^2(u - u_H)\|^2 \lesssim \|H^2 f\|^2 + \sum_{E \in \mathcal{F}(T)} |E| \, \|[D_{\mathrm{NC}}^2 u_h]_E \tau_E\|_{L^2(E)}^2$$
$$\lesssim \|H^2 f\|^2 + \|D_{\mathrm{NC}}^2(u_h - u_H)\|^2.$$

Thus, there exists some constant $c < 1$ such that

$$c\|D^2_{\mathrm{NC}}(u - u_H)\|^2 \le \|H^2 f\|^2 + \|D^2_{\mathrm{NC}}(u_h - u_H)\|^2.$$

The quasi-orthogonality of Lemma 2.1 and the Young inequality for any $0 < \alpha < c/C_{\mathrm{qo}}$ yield

$$\begin{aligned}
&\|D^2_{\mathrm{NC}}(u_h - u_H)\|^2 \\
&= \|D^2_{\mathrm{NC}}(u - u_H)\|^2 - \|D^2_{\mathrm{NC}}(u - u_h)\|^2 - 2(D^2_{\mathrm{NC}}(u - u_h), D^2_{\mathrm{NC}}(u_h - u_H))_{L^2(\Omega)} \\
&\le \|D^2_{\mathrm{NC}}(u - u_H)\|^2 - (1 - \alpha C_{\mathrm{qo}})\|D^2_{\mathrm{NC}}(u - u_h)\|^2 + C_{\mathrm{qo}}/\alpha\|H^2 f\|^2.
\end{aligned}$$

The combination of the foregoing two displayed inequalities shows

$$c\,\|D^2_{\mathrm{NC}}(u - u_H)\|^2 \le \|D^2_{\mathrm{NC}}(u - u_H)\|^2 - (1 - \alpha C_{\mathrm{qo}})\|D^2_{\mathrm{NC}}(u - u_h)\|^2 + (1 + C_{\mathrm{qo}}/\alpha)\|H^2 f\|^2.$$

This is equivalent to

$$\|D^2_{\mathrm{NC}}(u - u_h)\|^2 \le \frac{1 - c}{1 - \alpha C_{\mathrm{qo}}}\,\|D^2_{\mathrm{NC}}(u - u_H)\|^2 + \frac{\alpha + C_{\mathrm{qo}}}{\alpha(1 - \alpha C_{\mathrm{qo}})}\,\|H^2 f\|^2.$$

Any choice of $\alpha < c/C_{\mathrm{qo}}$ leads to $\rho := (1 - c)/(1 - \alpha C_{\mathrm{qo}}) < 1$ and

$$\|D^2_{\mathrm{NC}}(u - u_h)\|^2 \le \rho\,\|D^2_{\mathrm{NC}}(u - u_H)\|^2 + \frac{\alpha + C_{\mathrm{qo}}}{\alpha(1 - \alpha C_{\mathrm{qo}})}\,\|H^2 f\|^2.$$

3. Hierarchical A Posteriori Error Control

The hierarchical error control through (1.3) is established in this section for the Morley finite element scheme for the biharmonic equation in the notation of the previous section. Let

$$\eta := \|D^2_{\mathrm{NC}}(u_h - u_H)\| \quad \text{and} \quad \mu := \|H^2 f\| \tag{3.1}$$

with the right-hand side $f \in L^2(\Omega)$ and its oscillations with respect to the mesh $\mathcal{T}_H$, namely

$$\mathrm{osc}(f, \mathcal{T}_H) := \|H(f - \Pi_{0,H} f)\|.$$

The saturation property implies the reliability of the hierarchical error estimator $\eta + \mu$ and efficiency up to data oscillations.

Theorem A (hierarchical error control) *Let $\mathcal{T}_h \in \mathbb{T}$ be a uniform refinement of the regular triangulation $\mathcal{T}_H \in \mathbb{T}$. Then the error estimator $\eta + \mu$ defined in (3.1) is reliable and efficient in the sense that*

$$\|D^2_{\mathrm{NC}}(u - u_H)\| \lesssim \eta + \mu \lesssim \|(1 - \Pi_{0,H})D^2_{\mathrm{NC}} u\| + \mathrm{osc}(f, \mathcal{T}_H).$$

Proof. The combination of the saturation property from Theorem 2.1 with the Young and triangle inequalities proves for any $\delta > 0$ that

$$\begin{aligned}
\|D^2_{\mathrm{NC}}(u - u_H)\|^2 &\le (1 + \delta/2)\|D^2_{\mathrm{NC}}(u - u_h)\|^2 + (1 + 1/(2\delta))\|D^2_{\mathrm{NC}}(u_h - u_H)\|^2 \\
&\le (1 + \delta/2)\left(\rho\|D^2_{\mathrm{NC}}(u - u_H)\|^2 + C\|H^2 f\|^2\right) \\
&\quad + (1 + 1/(2\delta))\|D^2_{\mathrm{NC}}(u_h - u_H)\|^2.
\end{aligned}$$

The choice of sufficiently small δ such that $(1 + \delta/2)\rho < 1$ implies

$$\|D^2_{\mathrm{NC}}(u - u_H)\| \lesssim \|D^2_{\mathrm{NC}}(u_h - u_H)\| + \|H^2 f\|.$$

This proves the reliability. The efficiency of the term $\|H^2 f\|$ is proved in [1, 19, 29]. The efficiency of the hierarchical error estimator therefore follows from the triangle inequality and the best-approximation property from [16]

$$\|D^2_{\mathrm{NC}}(u - u_H)\| \lesssim \|(1 - \Pi_{0,H})D^2_{\mathrm{NC}}u\| + \mathrm{osc}(f, \mathcal{T}_H), \quad \text{and}$$
$$\|D^2_{\mathrm{NC}}(u - u_h)\| \lesssim \|(1 - \Pi_{0,h})D^2_{\mathrm{NC}}u\| + \mathrm{osc}(f, \mathcal{T}_h).$$

Remark 3.1. [other mesh-refinement strategies] The notion of uniform refinement in the main theorems is quite general in that it only requires bisection of edges in the triangulations which preserves the shape-regularity. Corresponding results for conforming FEMs [7] require newest-vertex bisection or red-green-blue refinement and have to avoid special mesh configurations. The result in this paper can dispense with any restriction on the mesh.

4. Numerical Experiments

The aim of this section is to gain empirical insight in the efficiency index of the hierarchical error estimator and the performance of adaptive mesh refinement driven by the local contributions of the hierarchical error estimator.
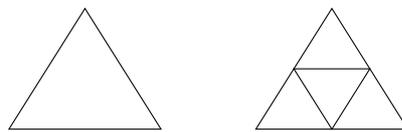
Figure 4.1. Red-refinement of a triangle.
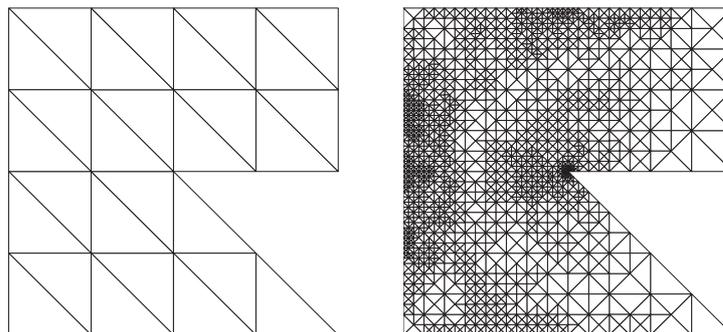
Figure 4.2. Left: initial mesh. Right: adaptive mesh generated by AFEM Variant 2 in level 10 of the adaptive loop; the number of triangles is 2730.

4.1. Numerical Realization

Consider the domain $\Omega = (-1,1)^2 \setminus (\mathrm{conv}\{(0,0),(1,-1),(1,0)\})$. Define $\omega := 7\pi/4$ and $\alpha := 0.50500969$. The exact singular solution [15] is given in polar coordinates by

$$u(r,\theta) = (r^2 \cos^2 \theta - 1)^2 \, (r^2 \sin^2 \theta - 1)^2 \, r^{1+\alpha} \, g(\theta)$$

for

$$g(\theta) = \left[\frac{\sin((\alpha-1)\omega)}{\alpha-1} - \frac{\sin((\alpha+1)\omega)}{\alpha+1} \right] \big(\cos((\alpha-1)\theta) - \cos((\alpha+1)\theta) \big)$$
$$- \left[\frac{\sin((\alpha-1)\theta)}{\alpha-1} - \frac{\sin((\alpha+1)\theta)}{\alpha+1} \right] \big(\cos((\alpha-1)\omega) - \cos((\alpha+1)\omega) \big).$$

The initial mesh is displayed in Figure 4.2. The hierarchical error estimator is computed with respect to one red-refinement, where each triangle is subdivided into four congruent children as depicted in Figure 4.1. The utilized Matlab programs for the Morley finite element method are described in [6].

4.2. Uniform Mesh Refinement

On a sequence of quasi-uniform meshes, the error estimator contribution μ is higher order compared to the error $u - u_H$ measured in the discrete energy norm. Figure 4.3 displays the convergence of the error and the error estimator contributions with respect to the number of degrees of freedom. The convergence rate is observed to be suboptimal. Figure 4.4 displays the efficiency indices. The ratio of $(\eta + \mu)$ and the true energy error lies between 0.8 and 0.9. The quotient of η and the true error is between 0.7 and 0.9. The efficiency index for μ converges to zero, which reflects the fact that μ is of higher order for uniform meshes.
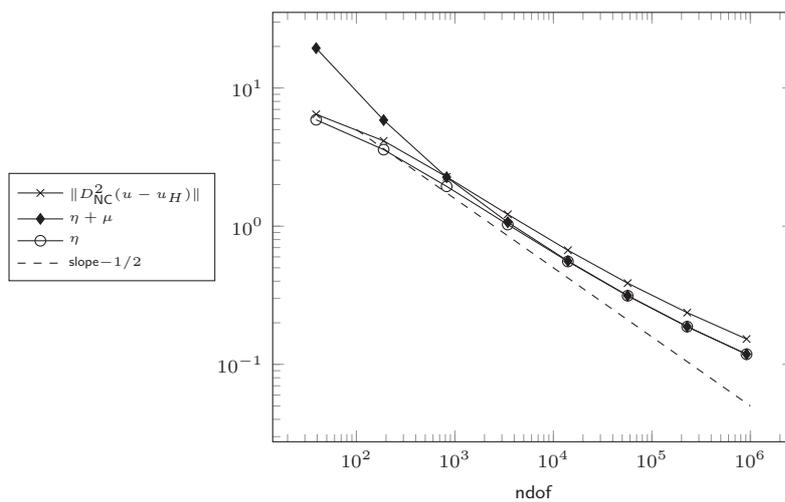
Figure 4.3. Convergence history for uniform mesh-refinement.
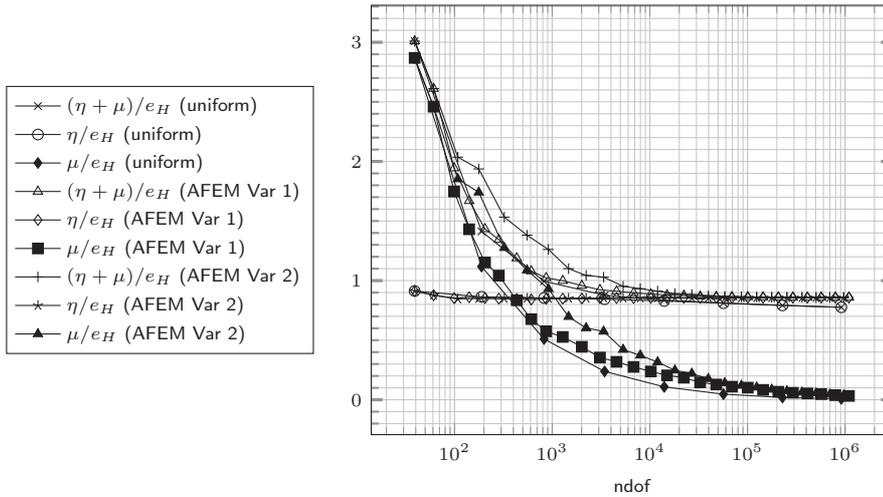
Figure 4.4. Efficiency indices for uniform mesh-refinement, adaptive mesh-refinement (Variant 1) and adaptive mesh-refinement (Variant 2) with $e_H := \|D_{\mathrm{NC}}^2(u - u_H)\|$.

INPUT. $\mathcal{T}_0 \in \mathbb{T}$ and $0 < \theta \leq 1$

FOR $\ell = 0, 1, 2, \ldots$

> SOLVE. Set $\mathcal{T}_H := \mathcal{T}_\ell$ and compute Morley FEM solution $u_H \in M(\mathcal{T}_H)$.
>
> ESTIMATE. Compute Morley FEM solution $u_h \in M(\mathcal{T}_h)$ on a uniform refinement $\mathcal{T}_h$ of $\mathcal{T}_H$ and local error estimator contributions $\eta_\ell^2(T)$, $\mu_\ell^2(T)$ for all $T \in \mathcal{T}_H$.
>
> MARK. Compute a subset $\mathcal{M} \subseteq \mathcal{T}_\ell$ of (almost) minimal cardinality such that
>
> $$\theta \sum_{T \in \mathcal{T}_\ell} (\eta_\ell^2(T) + \mu_\ell^2(T)) \leq \sum_{T \in \mathcal{M}} (\eta_\ell^2(T) + \mu_\ell^2(T)); \qquad \text{(Variant 1)}$$
>
> $$\theta \sum_{T \in \mathcal{T}_\ell} \eta_\ell^2(T) \leq \sum_{T \in \mathcal{M}} \eta_\ell^2(T). \qquad \text{(Variant 2)}$$
>
> REFINE. Compute a refinement $\mathcal{T}_{\ell+1}$ of $\mathcal{T}_\ell$ of minimal cardinality such that $\mathcal{M} \cap \mathcal{T}_{\ell+1} = \emptyset$ using newest-vertex bisection [2, 28].

END FOR

OUTPUT. Sequences of finite element solutions and meshes.

Figure 4.5. The adaptive algorithm in its two variants.

4.3. Adaptive Mesh Refinement

The numerical experiments in this subsection are devoted to the empirical study of the performance of self-adapted mesh-refinement based on the following refinement indicators, defined for any $T \in \mathcal{T}_H$ by

$$\eta_\ell^2(T) := \|D_{\mathrm{NC}}^2(u_h - u_H)\|_{L^2(T)}^2 \quad \text{and} \quad \mu_\ell^2(T) := \|H^2 f\|_{L^2(T)}^2.$$

For a given marking parameter $0 < \theta \leq 1$, the adaptive finite element method (AFEM) starts from a coarse initial triangulation $\mathcal{T}_0$ and runs the loop from Figure 4.5. In the experiments,
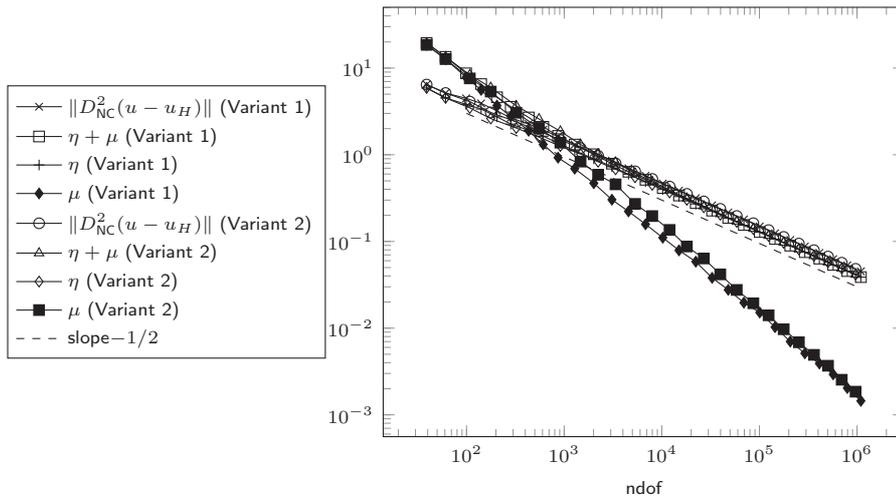
Figure 4.6. Convergence history plot for adaptive mesh-refinement.

the bulk parameter is $\theta = 0.3$. In Variant 1, the local contributions of $\eta_\ell^2(T) + \mu_\ell^2(T)$ are used as refinement indicators for the Dörfler marking [11]. In Variant 2, only the local contributions of $\eta_\ell^2(T)$ are used as refinement indicators. Figure 4.2 displays an adaptive mesh generated by Variant 2. Figure 4.6 displays the convergence of the error and the error estimator contributions with respect to the number of degrees of freedom. The convergence rate is observed to be optimal for both Variant 1 and Variant 2. The efficiency indices are displayed in Figure 4.4. The efficiency indices of μ are larger than in the case of uniform-mesh refinement, but seem converge to zero also in this case.

5. Saturation for the Crouzeix-Raviart FEM

This section briefly discusses the saturation (1.1) for the nonconforming Crouzeix-Raviart discretisation of the second-order Laplace equation. Given $f \in L^2(\Omega)$, the Poisson model problem seeks $u \in H_0^1(\Omega)$ with

$$(\nabla u, \nabla v)_{L^2(\Omega)} = (f, v)_{L^2(\Omega)} \quad \text{for all } v \in H_0^1(\Omega).$$

Given a regular triangulation $\mathcal{T}_h$ of Ω, the Crouzeix-Raviart finite element space reads

$$CR_0^1(\mathcal{T}_h) := \left\{ v \in P_1(\mathcal{T}_h) \,\middle|\, \begin{array}{l} v \text{ is continuous at the interior edges' midpoints} \\ \text{and vanishes at the midpoints of the edges of } \partial\Omega \end{array} \right\}.$$

The nonconforming FEM seeks $u_h \in CR_0^1(\mathcal{T}_h)$ such that

$$(\nabla_{\text{NC}} u_h, \nabla_{\text{NC}} v_h)_{L^2(\Omega)} = (f, v_h)_{L^2(\Omega)} \quad \text{for all } v_h \in CR_0^1(\mathcal{T}_h).$$

A direct extension of the results of this paper to the nonconforming P_1 FEM for the Poisson problem leads to the following result–the proof is omitted for brevity.

Theorem B. *There exist mesh-size independent constants $0 < \rho < 1$ and $0 < C < \infty$ such that the following holds. Let $\mathcal{T}_h \in \mathbb{T}$ be a uniform refinement of the regular triangulation $\mathcal{T}_H \in \mathbb{T}$*

with mesh-size function $H \in P_0(\mathfrak{T}_H)$. The discrete solutions $u_H \in CR_0^1(\mathfrak{T}_H)$ and $u_h \in CR_0^1(\mathfrak{T}_h)$ satisfy

$$\|\nabla_{\mathrm{NC}}(u - u_h)\|^2 \leq \rho \|\nabla_{\mathrm{NC}}(u - u_H)\|^2 + C \|Hf\|^2.$$

In contrast to Theorem 2.1, the data term in this estimate is *not* of higher order in general. However, in case that the solution is singular in the sense that $u \in H_0^1(\Omega) \setminus H^2(\Omega)$, the asymptotic convergence rate $O(h^\alpha)$ for some $\alpha < 1$ shows that the data term is indeed of higher order on uniform meshes and the saturation assumption is valid up to a higher-order term.

References

[1] L. Beirão da Veiga, J. Niiranen, and R. Stenberg, A posteriori error estimates for the Morley plate bending element, *Numer. Math.* **106**:2 (2007), 165–179.

[2] Peter Binev, Wolfgang Dahmen, and Ron DeVore, Adaptive finite element methods with convergence rates, *Numer. Math.* **97**:2 (2004), 219–268.

[3] H. Blum and R. Rannacher, On the boundary value problem of the biharmonic operator on domains with angular corners, *Math. Methods Appl. Sci.* **2**:4 (1980), 556–581.

[4] C. Carstensen and D. Gallistl, Guaranteed lower eigenvalue bounds for the biharmonic equation, *Numer. Math.* **126**:1 (2014), 33–51.

[5] C. Carstensen, D. Gallistl, and J. Gedicke, Justification of the saturation assumption, *Numer. Math.* **134** (2016), 1–25.

[6] C. Carstensen, D. Gallistl, and J. Hu, A discrete Helmholtz decomposition with Morley finite element functions and the optimality of adaptive finite element schemes, *Comput. Math. Appl.* **68**:12 (2014), 2167–2181.

[7] C. Carstensen, J. Gedicke, V. Mehrmann, and A. Międlar, An adaptive finite element method with asymptotic saturation for eigenvalue problems, *Numer. Math.* **128**:4 (2014), 615–634.

[8] C. Carstensen and R.H.W. Hoppe, Convergence analysis of an adaptive nonconforming finite element method, *Numer. Math.* **103**:2 (2006), 251–266.

[9] Chuanmiao Chen and Yunqing Huang, *High Accuracy Theory of Finite Element Methods*, Hunan science and technology press, Changsha, 1995 (in Chinese).

[10] Shaochun Chen, Mingfang Liu, and Zhonghua Qiao, An anisotropic nonconforming element for fourth order elliptic singular perturbation problem, *Int. J. Numer. Anal. Model.* **7**:4 (2010), 766–784.

[11] W. Dörfler, A convergent adaptive algorithm for Poisson's equation, *SIAM J. Numer. Anal.* **33** (1996), 1106–1124.

[12] Willy Dörfler and Ricardo H. Nochetto, Small data oscillation implies the saturation assumption, *Numer. Math.* **91**:1 (2002), 1–12.

[13] D. Gallistl, Morley finite element method for the eigenvalues of the biharmonic operator, *IMA J. Numer. Anal.* **35**:4 (2015), 1779–1811.

[14] P. Grisvard, *Elliptic problems in nonsmooth domains*, Monographs and Studies in Mathematics, vol. 24, Pitman, Boston, MA, 1985.

[15] P. Grisvard, *Singularities in Boundary Value Problems*, Recherches en Mathématiques Appliquées [Research in Applied Mathematics], vol. 22, Masson, Paris, 1992.

[16] T. Gudi, A new error analysis for discontinuous finite element methods for linear elliptic problems, *Math. Comp.* **79**:272 (2010), 2169–2189.

[17] J. Hu, Y.-Q. Huang, and Qun Lin, Lower bounds for eigenvalues of elliptic operators: by nonconforming finite element methods, *J. Sci. Comput.* **61**:1 (2014), 196–221.

[18] J. Hu and R. Ma, Superconvergence of both the Crouzeix–Raviart and Morley elements, *Numer. Math.* **132**:3 (2016), 491–509.

[19] J. Hu and Z.-C. Shi, A new a posteriori error estimate for the Morley element, *Numer. Math.* **112**:1 (2009), 25–40.

[20] J. Hu, Z.-C. Shi, and Jinchao Xu, Convergence and optimality of the adaptive Morley element method, *Numer. Math.* **121**:4 (2012), 731–752.

[21] P. Lascaux and P. Lesaint, Some nonconforming finite elements for the plate bending problem, *Rev. Française Automat. Informat. Recherche Operationnelle* **9**:R-1 (1975), 9–53.

[22] Q. Lin, H.-H. Xie, and Jinchao Xu, Lower bounds of the discretization error for piecewise polynomials, *Math. Comp.* **83**:285 (2014), 1–13.

[23] L. S. D. Morley, The triangular equilibrium element in the solution of plate bending problems, *Aeronaut. Quart.* **19** (1968), 149–169.

[24] T. K. Nilssen, X.-C. Tai, and R. Winther, A robust nonconforming H^2-element, Math. Comp. **70**:234 (2001), 489–505.

[25] R. Rannacher, Nonconforming finite element methods for eigenvalue problems in linear plate theory, *Numer. Math.* **33**:1 (1979), 23–42.

[26] D.-Y. Shi and P.-L. Xie, Morley type non-C^0 nonconforming rectangular plate finite elements on anisotropic meshes, *Numer. Methods Partial Differential Equations* **26**:3 (2010), 723–744.

[27] Z.-C. Shi, Error estimates for the Morley element, *Math. Numer. Sinica* **12**:2 (1990), 113–118.

[28] R. Stevenson, The completion of locally refined simplicial partitions created by bisection, *Math. Comp.* **77**:261 (2008), 227–241.

[29] R. Verfürth, *A Review of a Posteriori Error Estimation and Adaptive Mesh-Refinement Techniques*, Advances in Numerical Mathematics, Wiley, 1996.

[30] Y.-D. Yang, Z.-M. Zhang, and F.-B. Lin, Eigenvalue approximation from below using nonconforming finite elements, *Sci. China Math.* **53**:1 (2010), 137–150.